Numerical Modelling for Phase Change Materials

Alice Raeli
In collaboration with
M. Azaïez, M. Bergmann and A. Iollo

IMB – INSTITUT DE MATHÉMATIQUES DE BORDEAUX

CANUM 2016 - 9/13 May

Contents

Contents

Contents

Contents

Contents

Contents

Abengoa Solar - Sevilla, Spain

Renewable and Sustainable Energy : Solar Energy

Heliostats Area, solar power tower and salt tank (ABENGOA Solar-Sevilla Spain)

Hybrid Material

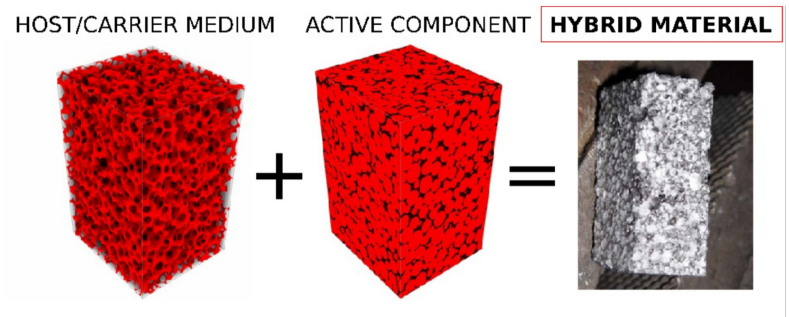

Hybrid Material, Graphite (G) and Salt (S)

Graphite ($\Longrightarrow$) Solid Phase

Molten Salt ($\Longrightarrow$) PCM Material (Solid, Liquid)

Problem Model

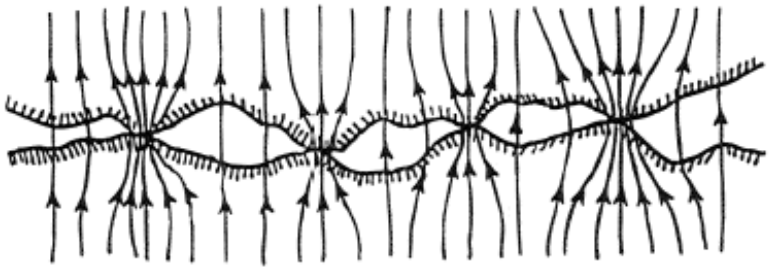

Interface Thermal Resistance $(\Longrightarrow)$ Jumps on u along the interface

$$(\kappa\partial_n u)_S = (\kappa\partial_n u)_G \qquad \text{Flux conservation}$$

$$R(\kappa\partial_n u)_G = (u_S - u_G) = [u] \qquad \text{Contact Resistance}$$

R : (Thermal) Contact Resistivity taken constant here.

$$-\mathrm{div}(\kappa(\vec{x}) \bigtriangledown u(\vec{x})) = g(\vec{x}), \qquad \text{in } G \cup S, \qquad (1a)$$

$$\kappa(\vec{x})\partial_{\vec{n}} u(\vec{x}) = 0, \qquad \text{on } \Gamma_N, \qquad (1b)$$

$$u(\vec{x}) = u_D(\vec{x}), \qquad \text{on } \Gamma_D, \qquad (1c)$$

$$[\kappa(\vec{x})\partial_{\vec{n}} u(\vec{x})] = 0, \quad R(\kappa\partial_{\vec{n}} u(\vec{x}))_S = [u], \qquad \text{on } \gamma \qquad (1d)$$

Spatial Discretization

Definition

The term *quadtree* is used in a more general sense to describe a class of hierarchical data structures whose common property is that they are based on the principle of recursive decomposition of space. They can be differentiated on the following bases:

- the type of data they are used to represent,
- the decomposition process,
- the resolution.

We call *cell or octant* the square/cube that it represents. Each cell may be the **parent** of four (eight in 3D) children. The **root** cell is the base of the tree and a **leaf** cell is a cell without any child. The **level** of a cell is defined by starting from zero for the root cell and by adding one every time a group of discendant children is added. Each cell C has two kinds of neighbours: through faces following the axial directions and through corner following its diagonals directions (edge concept is added in 3D).

To simplify the calculation and focus on certain types of meshes we add the balancing constraints:

- the levels of face neighbouring cells can not differ by more than one;
- the levels of diagonally neighbouring can not differ by more than two.

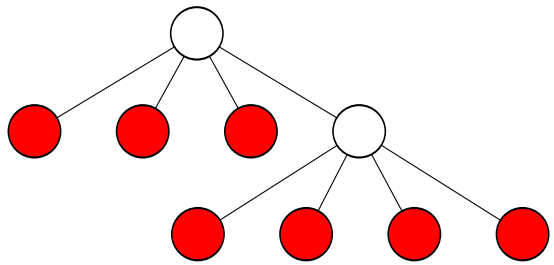

Figura: A linear quadtree representation.

The used tool for mesh refinement (PABLO `http://www.optimad.it/products/pablo/`) allows us to balance the tree working at the same time on non conforming grids. Moreover the used structure is a **linear octree**, so only the leafs data are stored with evident advantages in memory management.

To localize each cell this tool follows the Z-order and attribute to leafs the Morton Index. This procedure guarantee at the same time a localization in the space and a univoque characteristic identification on the cell itself.

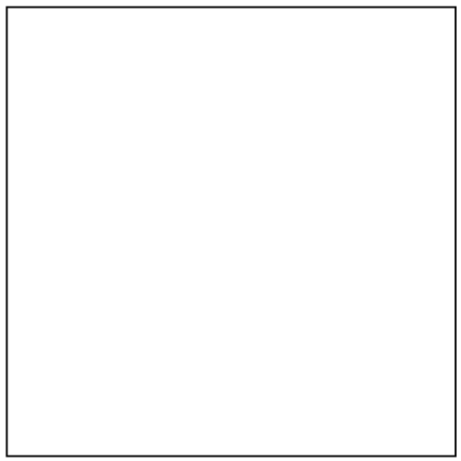

Let's consider a square domain being the root of our tree

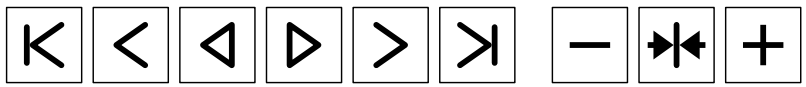

PABLO allows us to manage efficiently these structures and focus on the method to apply on cells neighbouring configurations. To each cell is attributed a univoque key that allows us to identify different configurations. We define a function of the level: $[L] := L - nL$, with L the level of the concerned octant and nL the level of the neighbour so that the value attributed to the key elements are:

0	♯ neighbours on this side
1	$[L] = 0$
2	$[L] = -1$
3	$[L] = 1$
4	$[L] = -2$
5	$[L] = 2$

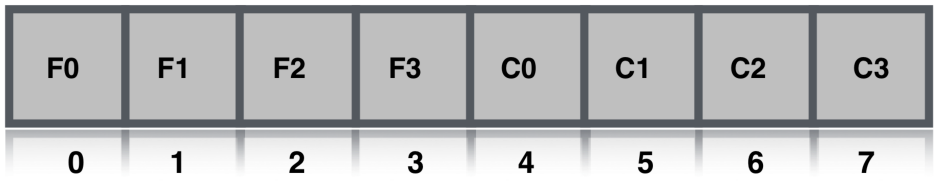

Remark

The processus to identify each configuration is repeated on three dimensional cases with an appropriate change of the variables number. The dimension of the key has to follow the possible neighbouring of the cube, so it will be a 26 digit array (at the place of 8) and go on for the other dimensions. Also the three dimensional configuration is Z-curve based, the order is shown in figure.

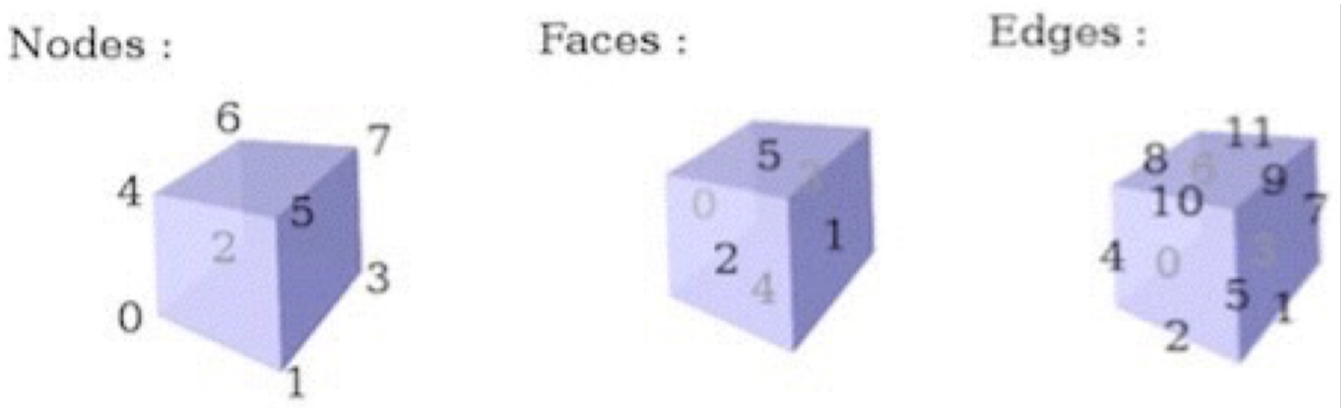

The Finite Difference Method

We consider a cell-centered finite difference method. We present a configuration test in figure.

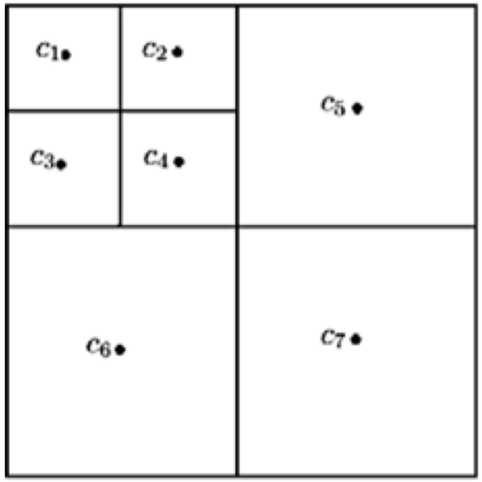

Theorem (Min et al., A supra-convergent finite difference scheme for the variable coefficient Poisson equation on non-graded grids.)

Considering a cell centered finite difference method on c_4, if only face-adjacent cells are to be used, then there does not exist any locally consistent linear scheme on nonuniform Cartesian grids.

We decided to extend the method involving all neighbours and not only the face adjacent cells. We develop a Taylor expansion for c_3 with respect to c_4, all the others points follow the same reason (u_i stands for the temperature calculated on point i):

$$u_3 = u_4 - h\frac{\partial u_4}{\partial x} + 0 * \frac{\partial u_4}{\partial y} + \frac{h^2}{2}\frac{\partial^2 u_4}{\partial x \partial x} + (zero \quad terms) + O(h^3)$$

A Taylor analysis complete on all the neighbours involved, with them relative linear combinations of the expansions, implies that the coefficients a_i must satisfy the following linear system:

$$\begin{pmatrix} 1 & 1 & 1 & 1 & 1 & 1 & 1 \\ 0 & -h & 0 & -h & \frac{3h}{2} & -\frac{h}{2} & \frac{3h}{2} \\ 0 & h & h & 0 & \frac{h}{2} & -\frac{3h}{2} & -\frac{3h}{2} \\ 0 & \frac{h^2}{2} & 0 & \frac{h^2}{2} & \frac{9h^2}{8} & \frac{h^2}{8} & \frac{9h^2}{8} \\ 0 & -h^2 & 0 & 0 & \frac{3h^2}{4} & \frac{3h^2}{4} & -\frac{9h^2}{4} \\ 0 & \frac{h^2}{2} & \frac{h^2}{2} & 0 & \frac{h^2}{8} & \frac{9h^2}{8} & \frac{9h^2}{8} \end{pmatrix} \begin{pmatrix} a_4 \\ a_1 \\ a_2 \\ a_3 \\ a_5 \\ a_6 \\ a_7 \end{pmatrix} = \begin{pmatrix} 0 \\ 0 \\ 0 \\ 1 \\ 0 \\ 1 \end{pmatrix}$$

In the example above the concerned points are seven so we can determine infinite solutions of the complete system but we search a unique one. The idea is to ensure consistency and, at the same time, to minimize the deviation from second-order accuracy. Let M be the constraints matrix, $\vec{a}$ the weights, $\vec{\lambda}$ the necessary additional unknowns, $\vec{f}$ the right hand side vector for consistency and $F(\vec{a})$ a weight function. The problem to minimize has the lagrangian form:

$$\mathcal{L} = F(\vec{a}) - \vec{\lambda}(M\vec{a} - \vec{f}) \tag{2}$$

We write minimization problem (2) in matrix form like:

$$Ax = b \Leftrightarrow \begin{cases} \frac{\partial F(\vec{a})}{\partial \vec{a}} - M^T\vec{\lambda} & = 0 \\ M\vec{a} & = \vec{f} \end{cases}$$

We call B the submatrix of consistency constraints and C the submatrix of order two constrains. Two cases have to be distinguished for N the number of concerned points in a configuration:

$N \leq 10 : \quad M = B$
$F(\vec{a}) = (1/2)\vec{a}^T(C^TC + \alpha I)\vec{a}$

$$Ax = \begin{pmatrix} ((1-\alpha)C^TC - \alpha I) & -B^T \\ B & 0 \end{pmatrix} x = b$$

The system satisfies 6 constraints for consistency and minimizes the second order constraints and the weights norm.

$N > 10 : \quad M = \binom{B}{C} \quad F(\vec{a}) = 1/2(\vec{a}^T\vec{a})$

$$Ax = \begin{pmatrix} I & -\binom{B}{C}^T \\ \binom{B}{C} & 0 \end{pmatrix} x = b$$

The system satisfies 10 constraints for second order accuracy and minimizes the weights norm.

Remark

With same reasons presented for the spatial discretization also for the method the three dimensional case follows the processus modifying properly the dimension of the system. We add the z direction, that means other 4 equation for the concistency and 6 for the second order. The two cases presented are so splitted in $N \leq 20$ and $N > 20$.

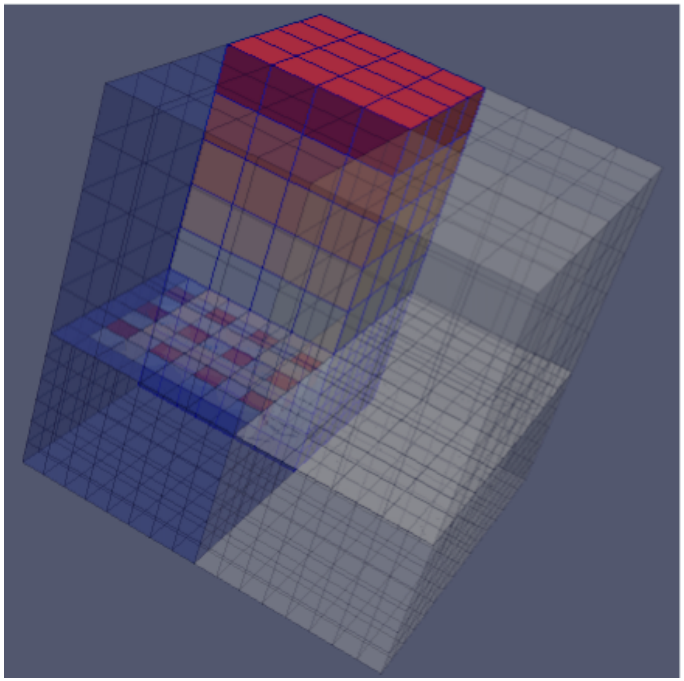

Figura: A parallel representation of a cube with one jump of level. Study of local consistency on the jump.

To check the consistency we reproduced the configuration presented above.

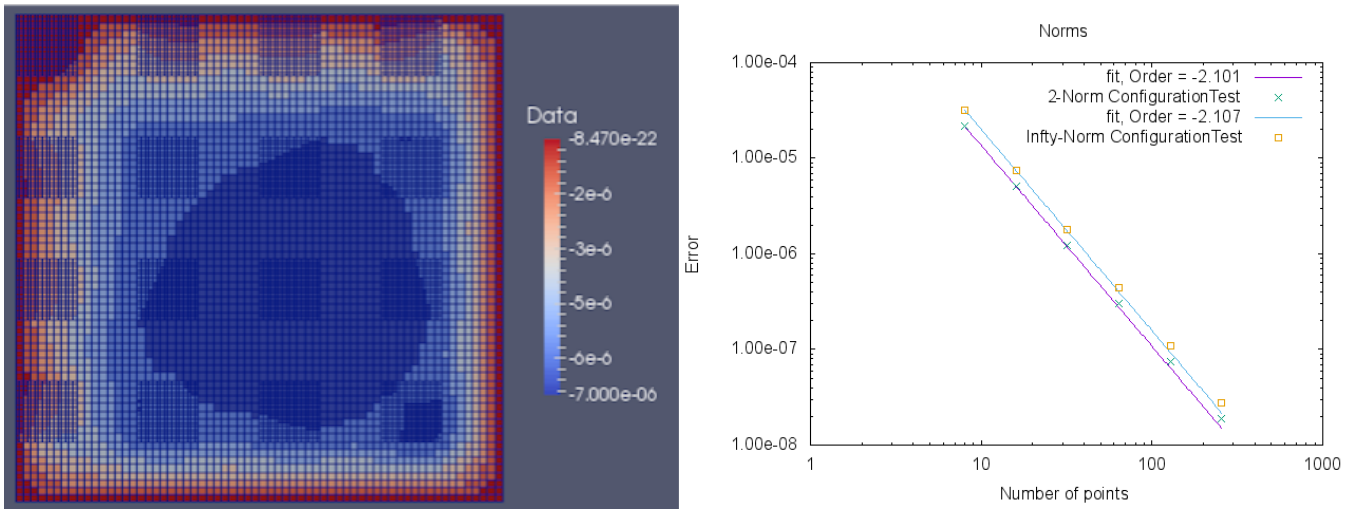

Figura: (Left) Error example, a concistency proof with increasing level for a laplacian of a sinusoidal function. (Right) Order study of the method on the test (logscale).

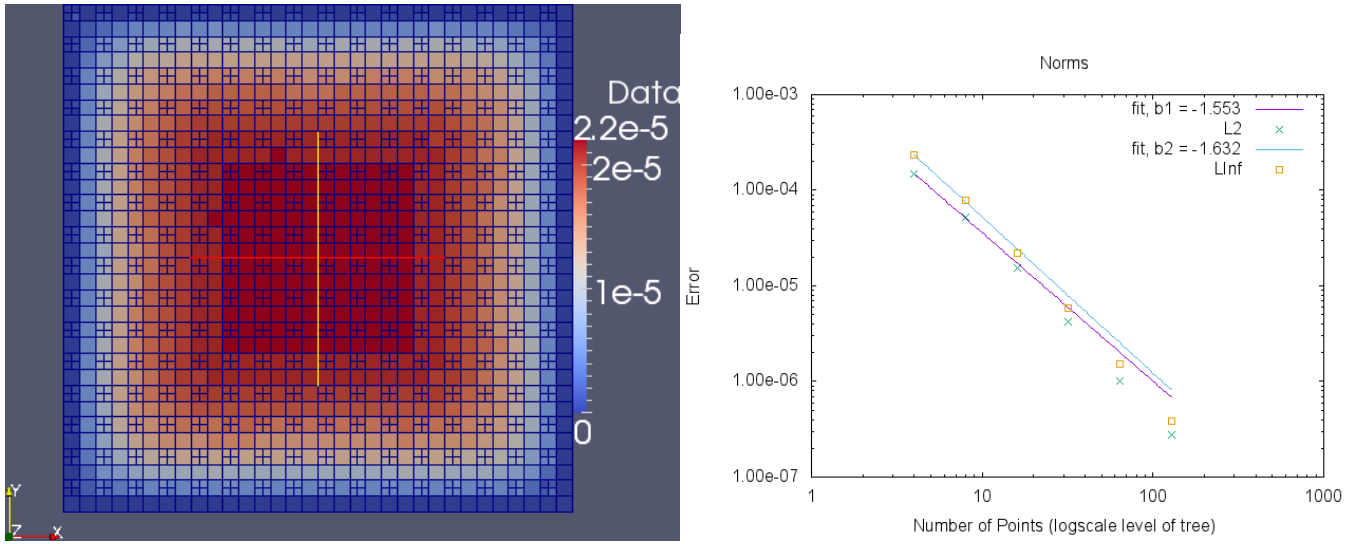

Figura: (Left) Alternative error example on the situation presented, concistency proof with increasing level for a laplacian of a sinusoidal function. (Right) Order study.

Tests and Results. Penalization

We approached the discontinuity simulation with more kinds of penalization tests that confirmed the theorical expectations.

$$\Delta u = g + \frac{\chi_c}{\varepsilon}(u - u_0) \tag{3}$$

Using u_0 constant value we introduce an error on boundary conditions. We penalized outside and inside the circle.

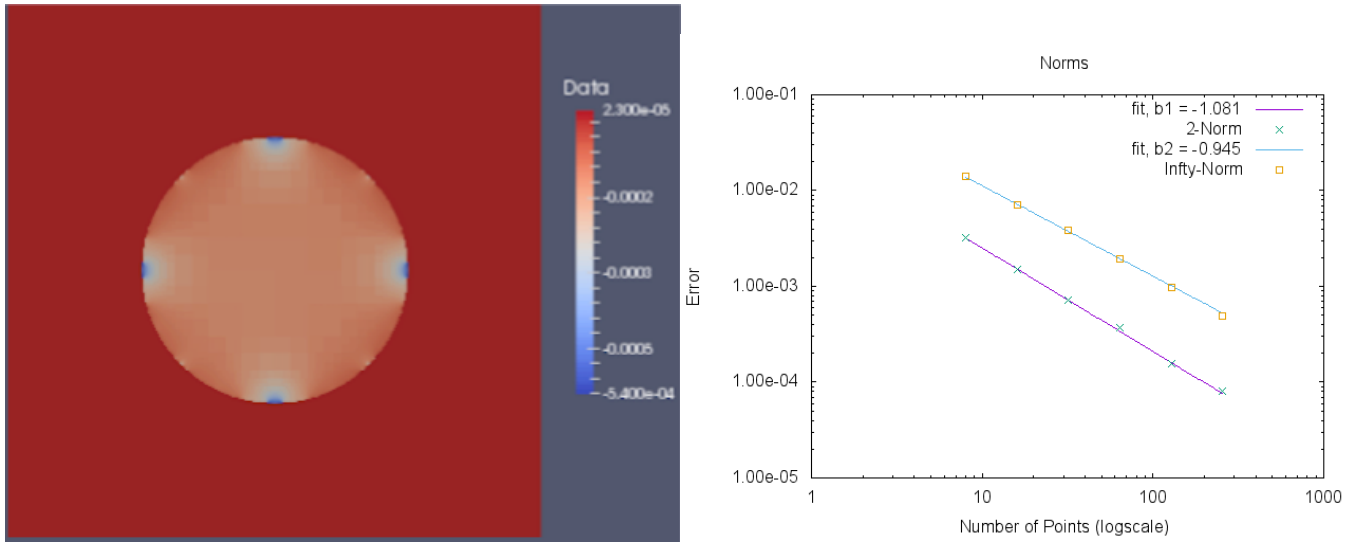

Figura: (Left) Error example, level of tree equal to 7 ($\Delta x = \Delta y = \frac{1}{2^7}$) (Right)Error order accuracy.

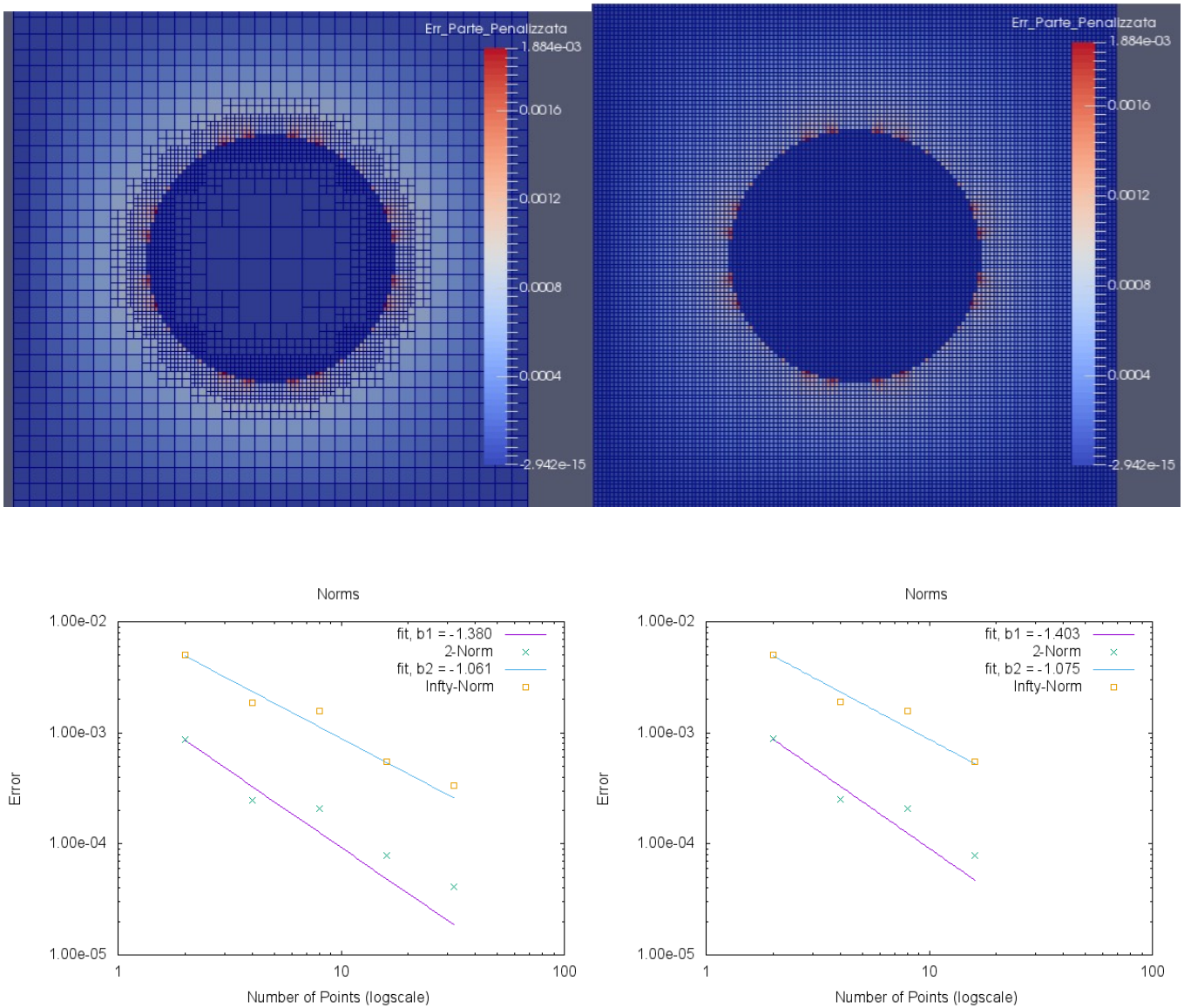

Figura: (a)-(b) Comparison between AMR and uniform mesh for the same error obtained at the same depth of the tree. (c)-(d) Error order study in both cases.

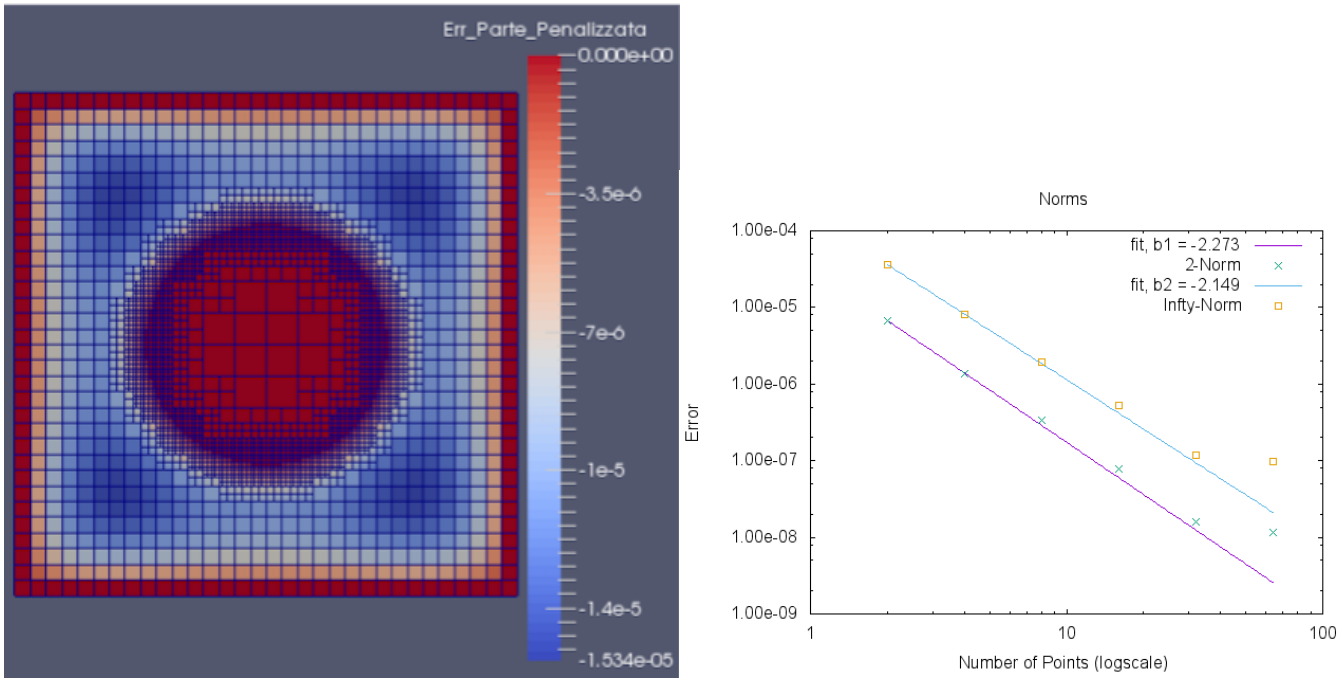

Figura: (Left) Error example with exact boundary condition imposed on the circle and its (Right) study of order accuracy.

AMR vs Uniform

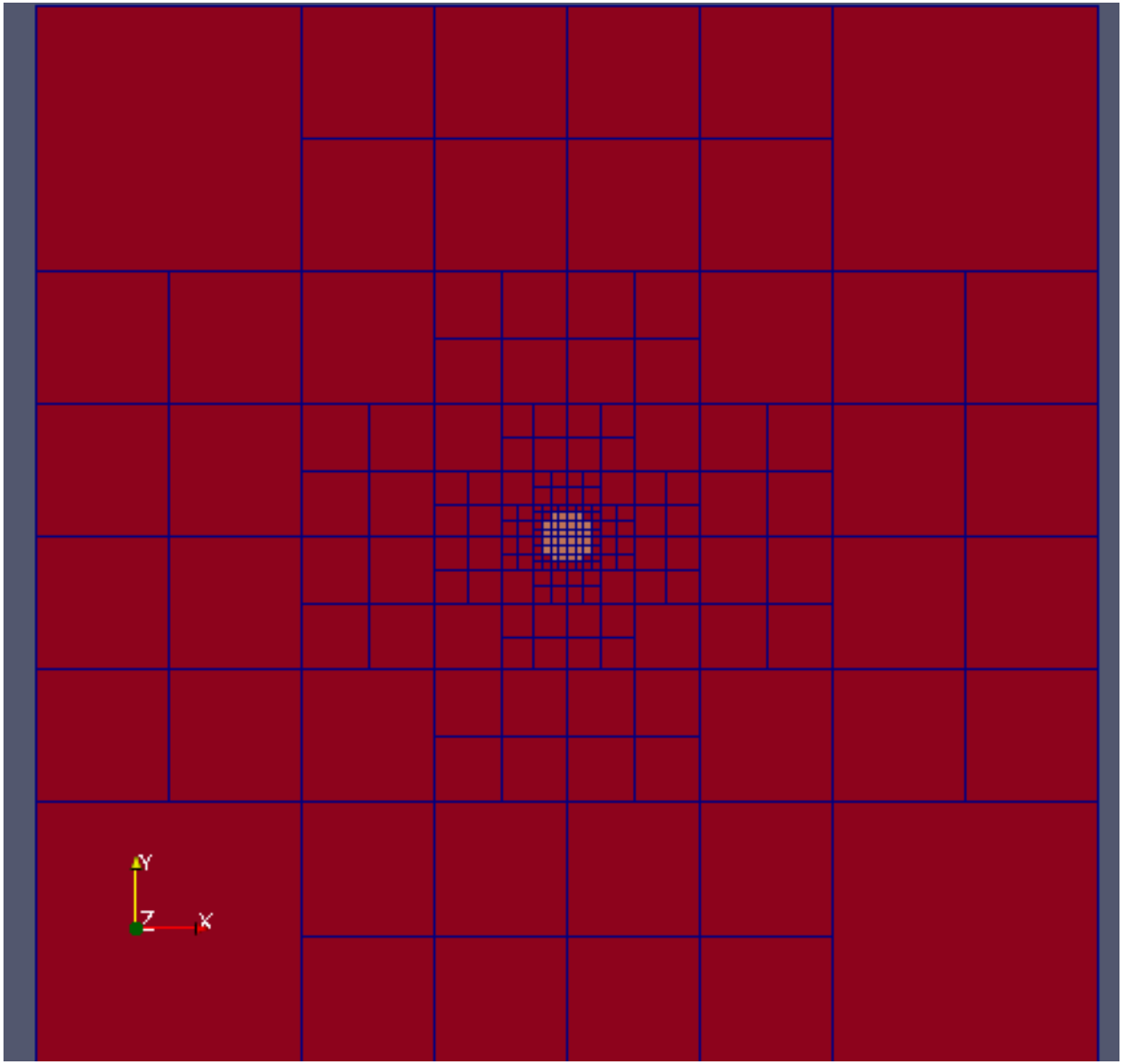

We compared the number of points between the mesh refinement on the penalized part and the uniform mesh. At the same error (sale depth of the tree) the gap becomes relevant in few passages.

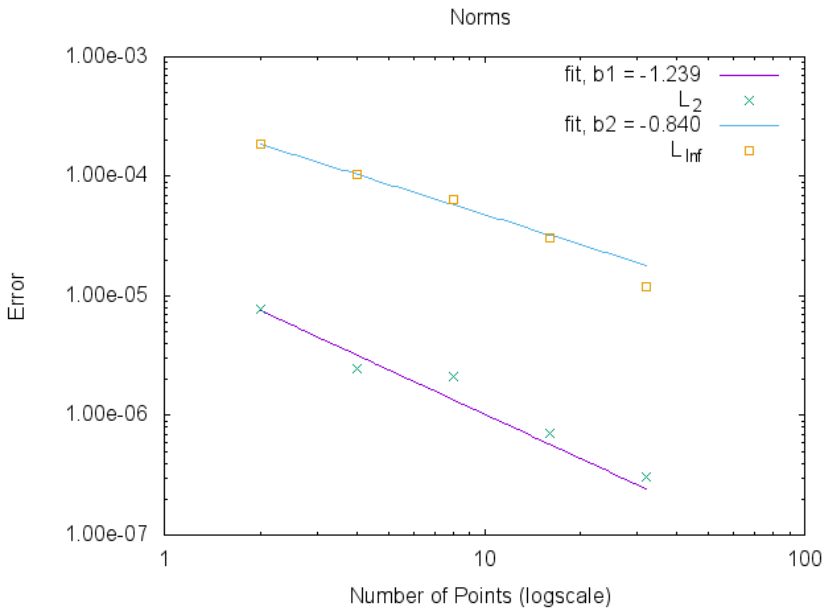

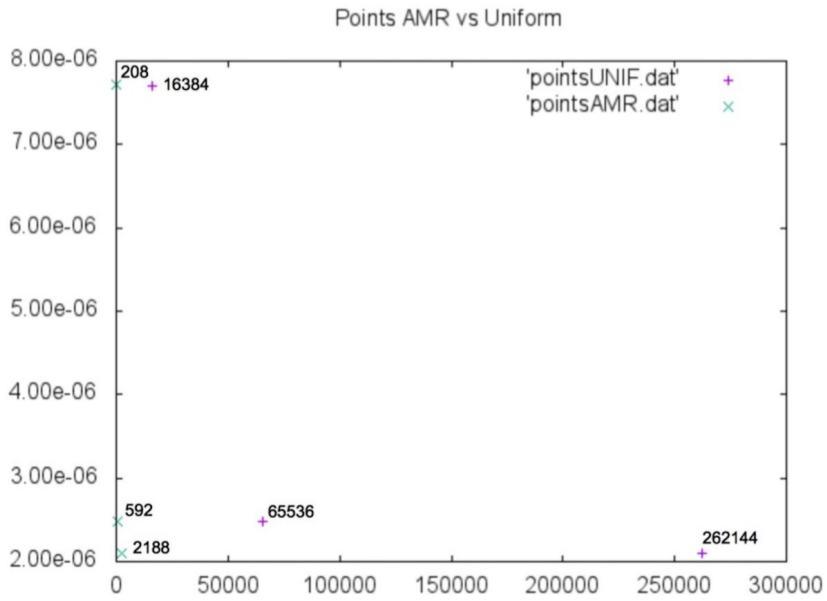

Discontinuity with mixed terms

$$\mathrm{div}(\kappa(\vec{x}) \bigtriangledown u(\vec{x})) = \tilde{f}(\vec{x})$$

$$u(\vec{x}) = \frac{1}{8} - \frac{1}{4} * ((x-0.5)^2 + (y-0.5)^2))$$

$$\tilde{f}(\vec{x}) = -\kappa(\vec{x}) + \kappa_x(\vec{x})u_x(\vec{x}) + \kappa_y(\vec{x})u_y(\vec{y})$$

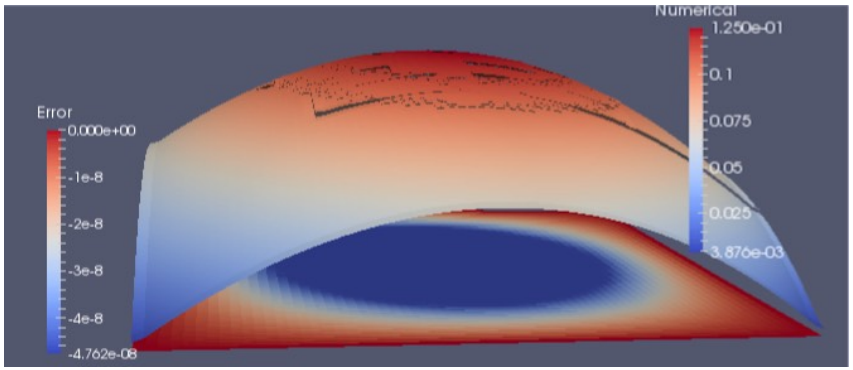

Figura: Error (bottom) and numerical solution obtained on AMR refinement for mixed terms equation.

$\kappa(\vec{x})$ from 1 to 1.000.000. We choose appropriate constants $A, B, Sharp$ and we define cell by cell $\kappa(\vec{x}) = (A+1) + B * \tanh(Sharp * C(\vec{x}))$, where $C(\vec{x})$ is an appropriate distance from the point to the level set of discontinuity (circular in the case presented).

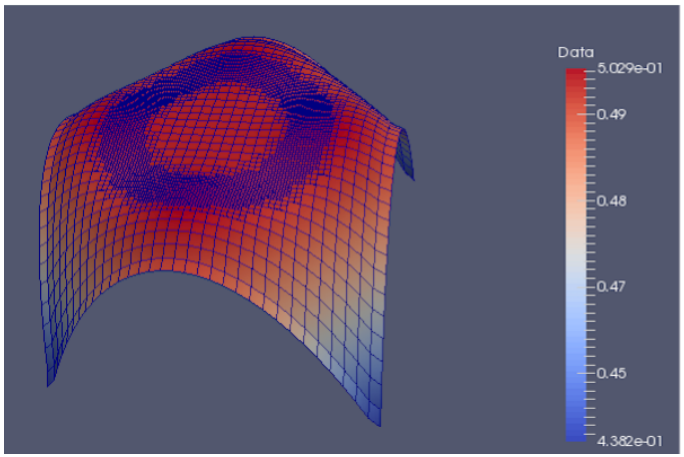

Figura: Penalization forced by the κ discontinuity if we impose $f(\vec{x}) = -1$

Three dimensional

3D sinus uniform

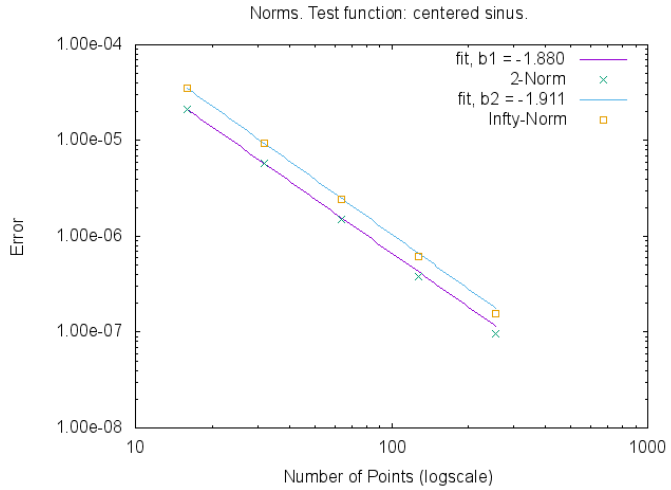

Grazie.